Mathematical Population Studies
Publication details, including instructions for authors and subscription information:
http://www.informaworld.com/smpp/title~content=t713644738

When a Collective Outcome Triggers a Rare Individual Event: A Mode of Metastatic Process in a Cell Population

MICHEL MALO[a]; AMANDINE CARTIER-MICHAUD[a]; ELISABETH FABRE-GUILLEVIN[ab]; GUILLAUME HUTZLER[a]; FRANCK DELAPLACE[a]; GEORGIA BARLOVATZ-MEIMON[ac]; ANNICK LESNE[de]

[a] IBISC FRE 3190 CNRS, Université d'Evry, Evry, France [b] Hôpital Georges Pompidou, Paris, France [c] Université Paris 12, Créteil, France [d] Institut des Hautes Études Scientifiques, Bures-sur-Yvette, Paris, France [e] LPTMC UMR 7600 CNRS, Université Pierre et Marie Curie, Paris, France

Online publication date: 05 August 2010

To cite this Article MALO, MICHEL , CARTIER-MICHAUD, AMANDINE , FABRE-GUILLEVIN, ELISABETH , HUTZLER, GUILLAUME , DELAPLACE, FRANCK , BARLOVATZ-MEIMON, GEORGIA and LESNE, ANNICK(2010) 'When a Collective Outcome Triggers a Rare Individual Event: A Mode of Metastatic Process in a Cell Population', Mathematical Population Studies, 17: 3, 136 — 165
To link to this Article: DOI: 10.1080/08898480.2010.490996
URL: http://dx.doi.org/10.1080/08898480.2010.490996

Mathematical Population Studies, 17:136–165, 2010

ISSN: 0889-8480 print/1547-724X online
DOI: 10.1080/08898480.2010.490996

Routledge
Taylor & Francis Group

When a Collective Outcome Triggers a Rare Individual Event: A Mode of Metastatic Process in a Cell Population

Michel Malo
Amandine Cartier-Michaud
IBISC FRE 3190 CNRS, Université d'Evry, Evry, France

Elisabeth Fabre-Guillevin
IBISC FRE 3190 CNRS, Université d'Evry, Evry and
Hôpital Georges Pompidou, Paris, France

Guillaume Hutzler
Franck Delaplace
IBISC FRE 3190 CNRS, Université d'Evry, Evry, France

Georgia Barlovatz-Meimon
IBISC FRE 3190 CNRS, Université d'Evry, Evry and
Université Paris 12, Créteil, France

Annick Lesne
Institut des Hautes Études Scientifiques, Bures-sur-Yvette, and
LPTMC UMR 7600 CNRS, Université Pierre et Marie Curie,
Paris, France

A model of early metastatic process is based on the role of the protein PAI-1, which at high enough extracellular concentration promotes the transition of cancer cells to a state prone to migration. This transition is described at the single cell level as a bi-stable switch associated with a subcritical bifurcation. In a multilevel reaction-diffusion scenario, the micro-environment of the tumor is modified by the proliferating cell population so as to push the concentration of PAI-1 above the bifurcation threshold. The formulation in terms of partial differential equations fails to capture spatio-temporal heterogeneity. Cellular-automata and agent-based simulations of cell populations support the hypothesis that a randomly localized accumulation of PAI-1 can arise and trigger the escape of a few isolated cells. Far away from the primary tumor, these cells experience a reverse transition back to a proliferative state and could generate a secondary tumor.

Address correspondence to Annick Lesne, LPTMC UMR 7600 CNRS, Université Pierre et Marie Curie, 4 place Jussieu, 75252, Paris, France. E-mail: lesne@lptmc.jussieu.fr

The suggested role of PAI-1 in controlling this metastatic cycle is candidate to explain its role in the progression of cancer.

Keywords: agent-based simulation; cell population; metastastic escape; multilevel model; multistability; reaction-diffusion

1. INTRODUCTION

Several modes of metastatic spreading (letting aside surgical dissemination) were identified: (i) transport in lymphatic circulation, (ii) transport in blood circulation, and (iii) a mode involving a specific migration mechanism, the *amoeboid migration* (Friedl, 2004). Taking place at the cell scale, the latter mode appears less pervasive than the first two ones, where circulation-facilitated transport spans the whole organism. However, it is less dependent on the anatomical features of the location of the tumor and is a candidate for the early events of the metastatic spreading before metastatic cells reach the lymphatic or the blood circulation. It might well be an essential preliminary step common to all metastatic processes.

A difficulty comes from the fact that early events involved in the escape of a cancer cell from the primary tumor are rare events, too rare to be easily observed or experimented in varying conditions. Only a small fraction of tumor cells provides the seeds for secondary tumors. Experimental protocols are restricted to indirect investigations, mainly genetic and biochemical analyzes of metastatic cells (Witz, 2008), or statistical tracking of the total number, location, and genetic lineage of secondary tumors (Albini, 2008). Experiments focus on the biochemical analysis of the surrounding micro-environment (Taylor et al., 2008), the morphological signature of potentially metastatic cells (Vincan et al., 2007), and the reproduction *in vitro* of the epithelial-mesenchymatous transition and the mesenchymatous-amoeboid transition which affect the morphology and the proliferative and migratory capacities (amoeboid migration) of cells of epithelial origin (Malo et al., 2006). These complementary experiments have shown that the metastatic process involves jointly genetic determinants (accumulation of specific mutations; Gerstung and Beerenwinkel, 2010/this issue), biochemical factors (triggering new pathways or switching existing ones, leading to modifications in the cell state and metabolism), and requirements about the state and geometry of the micro-environment—the extracellular space and matrix—of the tumor cells. However, there is no integrated understanding of this

process so far. The difficulty comes from the various potential causal factors, their locations and time scales, and is strengthened by the rarity of metastatic events. Modeling helps articulate the partial and indirect experimental results and interpret them in an integrated scenario, bridging molecular, cellular, extracellular, and cell population levels.

From biological facts about the mesenchymatous-amoeboid transition and amoeboid migration, we wish to explain how permissive conditions for the mestastatic escape of a few cancer cells might be collectively induced at the cell population level. Our claim is that proliferation-induced modifications of the tumor micro-environment could produce a feedback localized in a few privileged individual cells, selected by a complex conjunction of stochastic and history-dependent molecular events. Our working hypothesis, supported by experimental results (Malo et al., 2006), is the central role of the protein PAI-1, synthesized at high rate by the cancer cells and released in their immediate environment. We shall describe how this molecule could mediate an interplay between intra-cellular, extracellular, and cell population features, switching a few cells into a state prone to escape and migration, then switching them back into a proliferative state at a distance of the primary tumor (this is the process of metastasis). This scenario is rooted in a generic description of the single cell state in bifurcation theory, supported by *in vitro* experiments. Its spatially extended formulation at the cell population level is achieved in a reaction-diffusion model, implemented either in the standard framework of partial differential equations or in cellular automata and agent-based simulations. The predictions of our study motivated and guided new experiments proving the existence of the reverse change from the amoeboid to the mesenchymatous state. Finally, we use catastrophe theory to suggest a possible path toward the cancer stage where amoeboid state and migration can be observed.

2. BIOLOGICAL SETTING

Considering epithelial cells, a first transition toward a cancerous state is observed, originating in accumulating mutations and leading to the so-called *mesenchymatous state* (Figure 1, left). In this state, cell-cell junctions are no longer established and the epithelium is destabilized. This state has moreover a strong proliferative capacity; hence the transition to this mesenchymatous state is generally associated with the appearance of a well-defined tumor (Thiery, 2002). In invasive epithelial tumors, it is the default state of the cells (Gavert and Ben-Ze'ev, 2008), and it will be the default state of the cell population in our model.

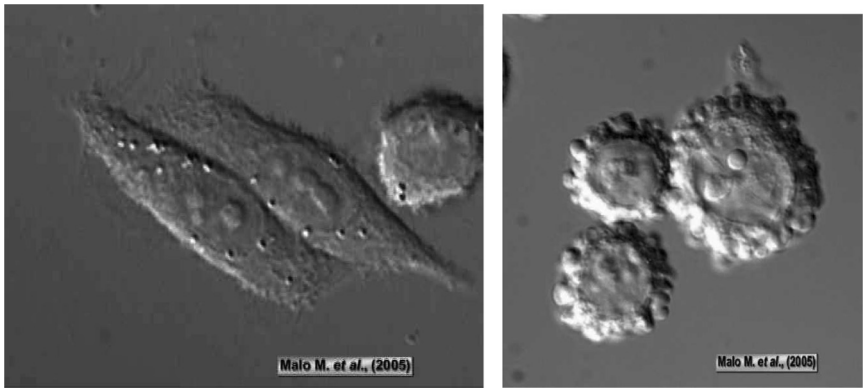

FIGURE 1 Epithelial cancer cells (colon cancer). (Left) Mesenchymatous state responsible for the destabilization of epithelium and prone to proliferation. (Right) Amoeboid state characterized by a bleb-shaped morphology and by modified adhesion leading to a special migratory ability. The mesenchymatous-amoeboid transition (as experienced by the rightmost cell in the left hand side picture) is likely to play a key role in early metastatic escape.

A second transition may occur toward the so-called *amoeboid state* (Figure 1, right) identified by a round shape with dynamic actin rings visible at the cell periphery. During this mesenchymatous-amoeboid transition, adhesion becomes integrin-independent, the actin cytoskeleton reorganizes, one of its regulatory pathways, RhoA-pathway, now involves an auxiliary protein, ROCK, and the proteolysis of the extracellular matrix ceases (Friedl, 2004; McCarthy, 2009). A bleb-shaped cell can move fast and progress by exploiting interstices of the substrate with no need of matrix proteolysis. Amoeboid migration is a very efficient mode of migration in a tissue, encountered in normal conditions during some developmental stages (Thiery, 2002); in a pathological context, Friedl and Wolf (2003) and Berx et al. (2007) suggested it as a privileged mode of metastatic migration.

In the mesenchymatous state, migration is inefficient while proliferation is very active. Proliferation is mostly controlled by cell density for steric reasons. In the amoeboid state, cell migration is very efficient. *Proliferation occurs at a high rate in the mesenchymatous state whereas migration occurs more efficiently in the amoeboid state*, in concordance with the mutual exclusion of proliferation and migration.

Recent observations *in vivo* hint at the role of the plasminogen-activator-inhibitor protein of type 1 (PAI-1) in amoeboid migration and in metastases. It is an ubiquitous species involved in several

pathways and functions, among which some aspects concern the metastatic process. It is found in the surroundings of the most invasive tumors (Pedersen, 2005; Wilkins-Port and Higgins, 2007; Wilkins-Port et al., 2007) and considered as a marker of bad prognosis (Jänicke et al., 2001; Look et al., 2002; Castello et al., 2007; Biermann et al., 2008). PAI-1 is encountered either as a newly synthesized molecule in the cell (*internal PAI-1*) or as a soluble form in the extracellular medium (*soluble PAI-1*). This latter form can diffuse in the extracellular medium, bind to the extracellular matrix (*matrix-bound PAI-1*), be trapped on the cell surface and deactivated, or be internalized and degraded with no further known consequence on the cell. In contrast, the internalization of matrix-bound PAI-1 occurs through the formation of a tripartite complex with a membrane receptor, uPAR, and a molecule, uPA. Its role in modifying the cell physiology (specifically, in modifying the activity of RhoA pathway) is acknowledged (Chazaud et al., 2000). When cancer cells are located on artificial substrates with high concentration $c_m > c_m^*$ of matrix-bound PAI-1, they experience the mesenchymatous-amoeboid transition (Malo et al., 2006). In this respect, matrix-bound PAI-1 can promote cancer cell migration, at least *in vitro* (Friedl and Wolf, 2003). Moreover, these experimental results, presented on Figure 2, indicate that the mesenchymatous-amoeboid transition is not due to some mutations but is rather a dynamic transition between two different states of the cell, controlled by its environment.

Cancer cells synthesize more PAI-1 than normal cells do; PAI-1 molecules are then secreted in the extracellular medium and can bind to the extracellular matrix in tumor boundary regions, where the matrix is not fully occupied by cells. Hence, the concentration of the matrix-bound PAI-1 in the border region of the tumor is expected to be higher than around normal cells. This was observed experimentally (Look et al., 2002; Chazaud et al., 2002). Cancer cells also produce more uPA and have an increased number of uPA membrane receptors uPAR, directly involved in the internalization of matrix-bound PAI-1. The net result is an *increased internalization flux* J_i *in cancer cells*, hence an amplification of the ensuing cell metabolic and morphological changes compared to normal cells.

In view of these experimental observations, our starting point will be the fact that a cancer cell, with regard to its metastatic potentialities, can be in either in the mesenchymatous or in the amoeboid state. We adopt the leading pattern according to which the abrupt mesenchymatous-amoeboid transition of a cell is controlled by its internalization flux of matrix-bound PAI-1. The coupled dynamics of several cells and extracellular medium have to be considered. Indeed, proliferation in the mesenchymatous state turns a single cell into an

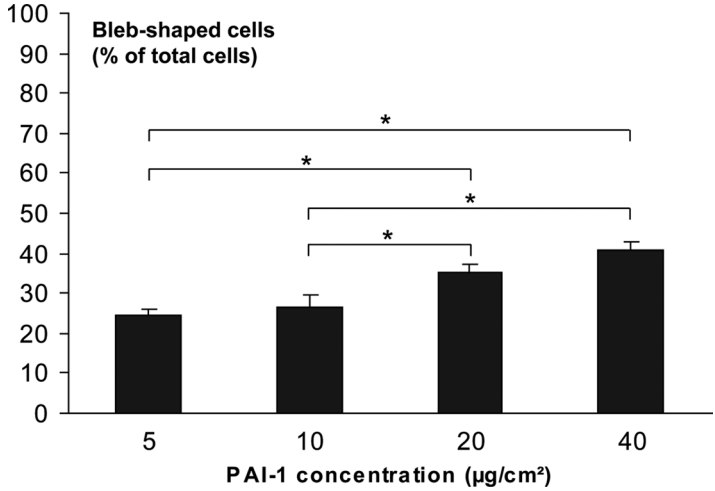

FIGURE 2 *In vitro* observation of the effect of the concentration of substrate-bound PAI-1 on cell morphology and the mesenchymatous-amoeboid transition. The proportion of MDA-MB-231 breast cancer bleb-shaped cells is measured at fixed PAI-1 concentration (values 5, 10, 20, 40 $\mu g/cm^2$); $^*p < 0.05$.

aggregate, collectively contributing to the concentration of matrix-bound PAI-1. We shall therefore embed the dynamics of a single cell in a spatially extended population model, focusing on the spatio-temporally varying internalization flux of the matrix-bound PAI-1, considered as a marker of the metastatic potentialities of the cells.

3. MODEL

3.1. Mechanisms

The mechanisms by which PAI-1 could play a role in the fate of cancer cells and in the metastatic process have functional consequences at four different levels:

- *At the molecular (intra-cellular) level*: internalization of matrix-bound PAI-1. The internalization of soluble PAI-1 has no intra-cellular consequences and amounts to a mere degradation;
- *At the cellular level*: mesenchymatous-amoeboid transition. The experimental fact that the concentration c_m of matrix-bound PAI-1 is a major determinant of the mesenchymatous-amoeboid transition (Figure 2) will be formulated in the framework of bifurcation theory

at the single cell level, with a control parameter related to c_m. The molecular analysis of intra-cellular pathways and morphological transformations shows that a more straightforward determinant of the mesenchymatous-amoeboid transition is the internalization flux J_i of the cell. Our hypothesis is that intra-cellular dynamics determining the overall cell state shows a bifurcation revealed by a switch between two markedly different mesenchymatous and amoeboid states, at some threshold value $J_i = J_i^*$;

- *At the cell population level*: the mutualized secretion of PAI-1, feeding extracellular PAI-1 species. Cell growth and division are considered at this level;
- *At the micro-environment level*: soluble PAI-1 diffusion in the extracellular medium and binding on the cell-free matrix, thus turning into matrix-bound PAI-1.

The point is to explain how the interplay between the various forms of PAI-1 and the various levels at which they are produced, controlled, or used can trigger the mesenchymatous-amoeboid transition and explain the metastatic process.

3.2. Reaction-Diffusion Model

We first consider a description (termed *mean-field-like description* in statistical physics for interacting many-body systems) in which species of soluble PAI-1, internal PAI-1, and matrix-bound PAI-1 are followed through their smooth deterministic concentrations. The cell population is characterized by a smooth deterministic cell density. The experimental observations are formalized in terms of chemical kinetics, diffusion, and growth, but the discrete nature of cells and molecules, and the stochasticity of the elementary processes are beyond the mean-field description. Variables include the concentrations $c_m(\vec{r},t)$ of matrix-bound PAI-1, $c_s(\vec{r},t)$ of soluble PAI-1, and $c_i(\vec{r},t)$ of internal PAI-1 at time t and location $\vec{r}$, and a smooth variable $\sigma(\vec{r},t)$ accounting for the presence of cells at $\vec{r}$. According to the standard continuous-medium approximation (Landau and Lifshitz, 1959), the element $d\vec{r}$ has to be large enough to contain a large number of molecules, so that concentrations are smooth and deterministic, but not too large so as to remain infinitesimal at the scale of the system. The concentrations are then ruled by chemical kinetic equations (mass action law) and by the diffusion equation (Fick law). Similarly, the variable σ is an homogenized version of the Boolean function $\sigma_0(\vec{r},t)$ with $\sigma_0(\vec{r},t) = 1$ if a cell is present in $\vec{r}$ at time t and 0 otherwise. There is need neither to count cells nor to care much for the boundaries of the

cell population, and the resulting cell density $\sigma(\vec{r},t)$ is a continuous field with $0 \leq \sigma \leq 1$. In particular, cell growth and cell division can be treated similarly, both producing a spreading of the support and a local increase of the field $\sigma(\vec{r},t)$. This description is mean-field insofar as correlations between the fluctuating numbers of molecules and cells at various locations and times are neglected and only their local averages are considered (Lesne, 2007). The overall dynamics is described in a spatially extended kinetic model, as illustrated on Figure 3, accounting for:

- *Cell division and growth*, continuously enlarging the region occupied by cells (where $\sigma > 0$). This expansion of the cell population is measured by a rate k_g and a unimodal kernel $\Gamma(\cdot)$ of finite range: cell growth and division induce a continuous spreading of the continuous regions with short-range increments weighted by Γ. As mentioned, there is no need to consider separate contributions for growth and division. This kernel is isotropic ($\Gamma(\vec{r})$ depends only on r), time-independent, normalized by setting to 1 its integral over the whole space. Its width corresponds to the cell radius;
- A source term describing the *synthesis of PAI-1* inside the cell. It describes the net result of the protein synthesis following gene expression, its degradation right after formation, and possibly a negative self-regulatory effect on the expression of PAI-1 gene. It is represented by a term $f(c_i)$ monotonously decreasing to 0 as the concentration c_i of internal PAI-1 increases, and such that $f(0) > 0$;

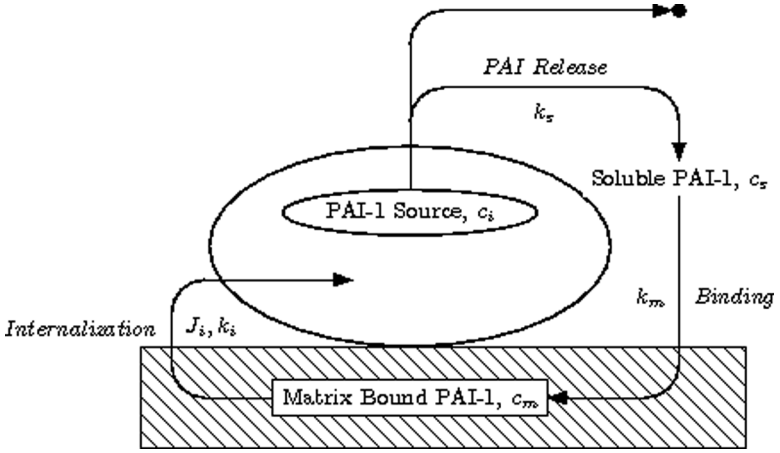

FIGURE 3 Fluxes and transformations of the three PAI-1 forms considered in the model.

- The *release of soluble PAI-1* when cells are present, feeding on their content in internal PAI-1. It is described by a pseudo-first-order kinetics, accounting only for the species of interest and the simple proportionality of the secreted amount with respect to c_i. The influence of possible additional factors and species other than PAI-1 is implicitly taken into account in the effective rate k_s;
- Soluble PAI-1 then *diffuses* with a diffusion coefficient D. The fact that it diffuses only in the extracellular medium is reflected by a space-dependent diffusion coefficient $(1-\sigma(\vec{r},t))D$ vanishing at maximal cell density $\sigma=1$;
- The *fixation* of soluble PAI-1 on the matrix when no cell is present, producing matrix-bound PAI-1 with a rate $(1-\sigma(\vec{r},t))k_m$ which vanishes at maximal cell density $\sigma=1$;
- The *deactivation* of soluble PAI-1 or its internalization; this process is much different from the internalization of matrix-bound PAI-1 with regard to cell physiology: it has no signaling role and does not trigger any pathway, having finally no consequence on the overall state of the cell; hence it should not be taken into account in the internalization flux J_i introduced as a control parameter of the mesenchymatous-amoeboid transition. Both deactivation and internalization merely amount to a degradation of soluble PAI-1 and are jointly accounted for by a first order kinetic $-\sigma k_d c_s$. They correspond to the only possible fate for soluble PAI-1 at maximal cell density, when $\sigma=1$ and diffusion or matrix-binding are no longer possible;
- The *internalization of matrix-bound PAI-1* with a rate k_i when a cell is present. This process generates the internalization flux J_i per cell, according to an effective single-order kinetics $J_i=k_i c_m$. As in first-order kinetic terms, the rate k_i is an effective parameter possibly depending on factors omitted in this basic model; only here the proportionality between the concentration c_m and the flux J_i matters. This flux triggers the mesenchymatous-amoeboid transition when it exceeds a threshold J_i^*. Internalized PAI-1 molecules are degraded after influencing internal pathways controlling the transition of the cell state.

In terms of regular deterministic fields, these different processes, individually well-established experimentally, lead to the system:

$$\begin{cases} \partial\sigma/\partial t = k_g H(1-\sigma) \int_{R^3} \sigma(\vec{r}')\Gamma(\vec{r}'-\vec{r})d\vec{r}' & (1)\\ \partial c_i/\partial t = \sigma f(c_i) - k_s \sigma c_i & (2)\\ \partial c_s/\partial t = (1-\sigma)D\Delta c_s + k_s\sigma c_i - k_m(1-\sigma)c_s - k_d\sigma c_s & (3)\\ \partial c_m/\partial t = k_m(1-\sigma)c_s - k_i\sigma c_m & (4)\\ J_i = k_i c_m \qquad \text{for } \sigma > 0, & (5) \end{cases}$$

where $H(\cdot)$ is the Heaviside step function such that $H(z)=1$ if $z>0$, and $H(z)=0$ otherwise. The intra-cellular synthesis and degradation of PAI-1 forbid the conservation of PAI-1 in the system.

Eq. (2) and the features of the function f show that $\partial c_i/\partial t$ is strictly positive for c_i close to 0 and that it decreases monotonously as c_i increases, reaching negative values for c_i large enough; we then expect to observe a stationary value $\bar{c}_i$ where cells are persistently present ($\sigma>0$). This $\bar{c}_i$ is the unique solution of $f(\bar{c}_i)=k_s\bar{c}_i$. In Eq. (3), the degradation term ensures that c_s remains bounded. In regions where $\sigma<1$, the diffusion term describes how the soluble PAI-1 produced by the tumor cells diffuses in the extracellular space toward the tumor boundary and beyond, in the outer shell, where it binds the extracellular matrix and increases the concentration of matrix-bound PAI-1, while c_s tends to 0 far away from the tumor in the regions not reached yet by the diffusion. Eq. (4) shows that $\partial c_m/\partial t<0$ in regions where cells are dense (σ close to 1) while $\partial c_m/\partial t<0$ at the tumor outer boundary, that is, in a region almost devoid of cells (σ close to 0) but not too far from the cells producing PAI-1, so that $c_s>0$. We expect that $c_m=0$ in the tumor bulk while reaching its maximum value in the tumor outer shell, before decreasing to 0 far away from the tumor: matrix-bound PAI-1 is mainly located in the tumor boundary regions where both σ and $1-\sigma$ are non zero. Core tumor cells can neither escape nor even move, *only tumor boundary regions are involved in the metastatic escape process*.

J_i given by Eq. (5) is defined as an internalization flux *per cell*. As the mesenchymatous-amoeboid transition occurs at the cell level, its relevant control parameter should correspond to a cell as a whole, notwithstanding its spatial extent. The question is to determine whether this flux J_i could exceed the transition threshold in some cells, that is, $J_i>J_i^*$ with $J_i^*=k_ic_m^*$. Such an occurrence requires the conjunction of the production of soluble PAI-1 by tumor cells, the diffusion of soluble PAI-1 in the vacant extracellular space, the binding of a large amount of soluble PAI-1 at a given empty location of the extracellular matrix, the growth or the division of a cell to cover this location, the internalization of the underlying matrix-bound PAI-1, and the experience of the mesenchymatous-amoeboid transition. This sequence of events is ordered: soluble PAI-1 binds the matrix and c_m reaches a high level *before* a cell invades the corresponding location. This heuristic analysis shows the importance of the precise spatio-temporal geometry of the tumor, the history of its growth, and the relative timing of the various events occurring at its boundary. Consistency and relevance of the approximations leading to Eq. (1)–(5) must be reevaluated.

Accounting for the constraint that soluble PAI-1 diffuses only in the extracellular medium imposes boundary conditions on the bare

diffusion equation (involving a bare diffusion term $D\Delta c_s$) delineating the space available for diffusion. However, cell division is a random event at the cellular level so that the tumor boundary itself is random and irregular. A precise account of the boundary conditions would require a full description of the random growth of the tumor and history of the cell population, hence the extension to a stochastic setting. On the contrary, Eq. (1)–(5) involve an average version σ of the actual Boolean function indicating where cells are present and account for the geometrical constraints through an *effective diffusion coefficient* $(1-\sigma)D$. This description ignores inhomogeneities, whose role however is reinforced by the heterogeneous growth and the geometry-dependent interplay between intra- and extra-cellular processes. This prevents the solution for c_m from reaching the very high level required to exceed the mesenchymatous-amoeboid transition threshold. Rough estimates from Eq. (2)–(4) in the outer shell where $\sigma \approx 1/2$ are the stationary and spatially uniform concentrations $c_i \approx \bar{c}_i$, $c_s \approx \bar{c}_s = k_s\bar{c}_i/(k_m + k_d)$ and $c_m \approx \bar{c}_m = k_m\bar{c}_s/k_i$: c_m either always or never exceeds the threshold c_m^* of the mesenchymatous-amoeboid transition, depending on the values of the kinetic rates in Eq. (1)–(5). Either all cells or none display the mesenchymatous-amoeboid transition and escape. This does not correspond to the metastatic process where only very few cells emerging spontaneously manage to escape.

The invasion by a new cell of an extracellular matrix site covered by PAI-1 is mainly a random event, but we consider here that it is fully controlled by a homogeneous and deterministic spreading of a smooth field $\sigma(\vec{r}, t)$: partial differential Eq. (1)–(5) ignore the geometry of the tumor boundary. A better model replacing the homogenized description through the field σ by an explicit description of the occupied region encounters singularities at the boundaries between cells and extracellular medium. It requires the introduction of regularizing kernels. Moreover, at this level of description, consistency asks for an explicit stochastic model for cell growth and division. These two difficulties generate too many parameters, to the detriment of robustness. We rather turn to a numerical modeling to represent the history of the tumor and its stochastic growth. Cellular-automata and agent-based simulations, completing one another help describe the interplay between the geometry of the tumor boundary and the accumulation of matrix-bound PAI-1.

3.3. Cellular-Automata and Agent-Based Simulations

In addition to implementing the same mechanisms as partial differential equations (Figure 3), the cellular-automata simulation reflects the

cell discreteness and the stochastic aspect of the cell division. It shows that stochastic variation in cell division and tumor growth are sufficient to produce the heterogeneous accumulation of matrix-bound PAI-1 at the tumor boundary. Agent-based simulation includes the action of vitronectine (a molecular species) and comprises more cell states.

Both simulations predict a heterogeneous accumulation of matrix-bound PAI-1, yielding supra-threshold concentration peaks, leading in turn to the high internalization fluxes of PAI-1 in novel cells reaching these very specific locations; in the ensuing step (not included in the simulations) these few cells experience the mesenchymatous-amoeboid transition and are plausible candidates for the metastatic escape.

3.3.1. *Cellular Automata*

Cellular automata reproduce the stochastic variation of the cell division and the spatial constraints on tumor growth. They help us decide whether or not c_m can reach the transition threshold c_m^* locally. The simulation takes place on a two-dimensional grid, where the spatial extent of each cancer cell corresponds to a unit grid cell (to avoid confusion between numerical cells of the simulation grid and biological cells of the tumor, we use the term "grid cell" for the former and simply "cells" for the latter). The concentrations c_i, c_s, and c_m are defined on the discrete space-time $\{(\vec{r},t) \in \mathbb{N}^2 \times \mathbb{N}\}$ and take any real positive value; $\sigma(\vec{r},t)$ defined on $\mathbb{N}^2 \times \mathbb{N}$ takes only values 0 or 1 according to the absence or presence of a cell in $\vec{r}$ at time t. The simulation is synchronous, the state of each grid cell is updated at each step. The growth of the tumor and the coupled variation of the different forms of PAI-1 (internal, soluble, and matrix-bound) are implemented according to the kinetic scheme described in Figure 3. An additional simplification consists of considering that c_i attains its stationary value $\bar{c}_i$ fast enough and $c_i = \bar{c}_i$ in all cells; k_s is replaced by an effective coefficient $k_{s,\text{eff}}$ (with the relationship $k_{s,\text{eff}} = k_s \bar{c}_i$ to the previous model). As we have no experimentally supported expression of the function f yet, the simplification $c_i = \bar{c}_i = \text{constant}$ restricts the influence of f to the value of $k_{s,\text{eff}}$. Keeping an equation for c_i with an unreliable term $f(c_i)$ is misleading. Omitting the argument $(\vec{r},t)$ in all right hand side quantities c_i, c_s, c_m, Δc_s, and σ, a basic step of simulation is:

$$\begin{cases} c_m(\vec{r},t+1) = c_m + k_m(1-\sigma)c_s - k_i \sigma c_m \\ c_s(\vec{r},t+1) = D(1-\sigma)\Delta c_s + k_{s,\text{eff}}\sigma + c_s(1 - k_m(1-\sigma) - k_d\sigma). \end{cases} \tag{6}$$

Denoting $\vec{r} = (x,y)$, the standard discretization of the Laplacian involved in describing the diffusion of soluble PAI-1 is:

$$\begin{aligned}\Delta c_s(x,y,t) = (1/4)(c_s(x+1,y,t) + c_s(x-1,y,t) \\ + c_s(x,y+1,t) + c_s(x,y-1,t)) - c_s(x,y,t).\end{aligned} \tag{7}$$

This implementation corresponds to a space-time discretization of the partial differential equations except for what concerns the growth of the tumor, now described as a stochastic process involving discrete cells: at each time step, one cell is created at the periphery of the tumor and its location is chosen at random among the empty sites around the tumor. At the beginning of the simulation, $c_m = 0$ and $c_s = 0$ for each grid cell, and one cell is located at the center of the grid. The internalization flux J_i is the control parameter of the mesenchymatous-amoeboid transition; namely, the transition occurs in a given cell when its flux J_i exceeds a threshold J_i^*. This overshoot is controlled directly by the concentration of matrix-bound PAI-1 at the location of the cell, established before a cell is created at this location. During the simulation, we record the spatio-temporal variation of the internalization flux and the various concentrations. We expect a realistic metastatic effect if the mean-field internalization flux $\overline{J}_i \approx k_i \bar{c}_m$ is below J_i^*: on average, the bifurcation threshold is not reached, otherwise most cells would experience the transition, a fact at odds with experimental observations. In this case, only a nontrivial localization could allow a few cells to encounter high enough levels of matrix-bound PAI-1. The resulting internalization is sufficient to display a mesenchymatous-amoeboid transition. Figure 4 shows the concentration of matrix-bound PAI after a trajectory of 500 simulated steps on a 40×40 cell grid. In concordance with our qualitative analysis, matrix-bound PAI-1 is mainly located at the tumor outer boundary. Several peaks appear at the periphery of the tumor; their locations vary from one simulation to another, and their heights are highly variable form place to place, with a standard deviation of the order of their mean value (Figure 5). On the tumor boundary, peaks are correlated with "gulfs," which favor the localized accumulation on a single site of PAI-1 produced by several neighboring cells.

The simulation shows that the interplay of transformation and degradation kinetics of PAI-1, the molecular diffusion of soluble PAI-1 secreted collectively by the tumor boundary cells in the extracellular medium, and the randomly changing geometry of the tumor can induce a localized accumulation of matrix-bound PAI-1 at a few path-dependent locations. It produces peaks in the flux J_i of internalization 1 by the cells of the matrix-bound PAI-1. The secretion of PAI-1

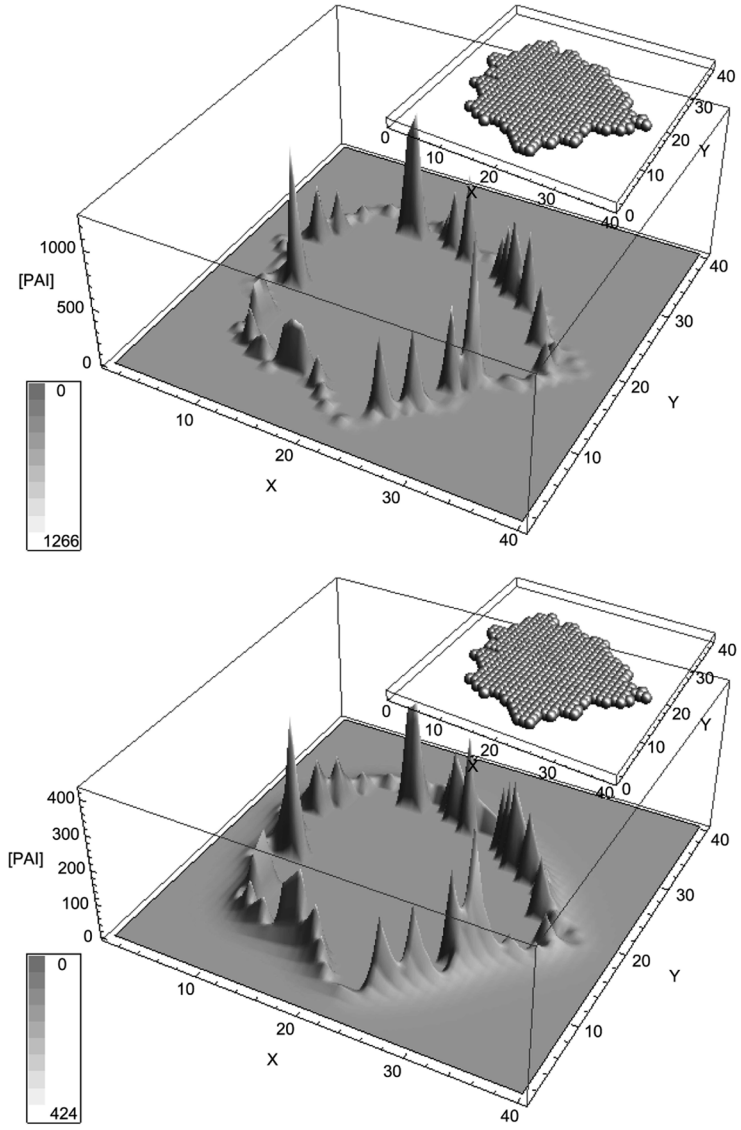

FIGURE 4 Concentration of matrix-bound PAI-1 (vertical axis) after 500 steps of simulation, starting from a null concentration in the whole unit square ($x \in [0, 1]$, $y \in [0, 1]$) and one tumor cell at the center, with $k_d = 0$, $k_i = 0.1$ and (top) $k_s = 1$, $k_m = 1$ or (bottom) $k_s = 0.5$, $k_m = 0.25$. The insets describe the corresponding shape of the tumor. In a wide range of values of k_m and k_s, matrix-bound PAI-1 displays a heterogeneous distribution, localized at the tumor boundary whose peaks correlate with the gulfs in the geometry of the boundary.

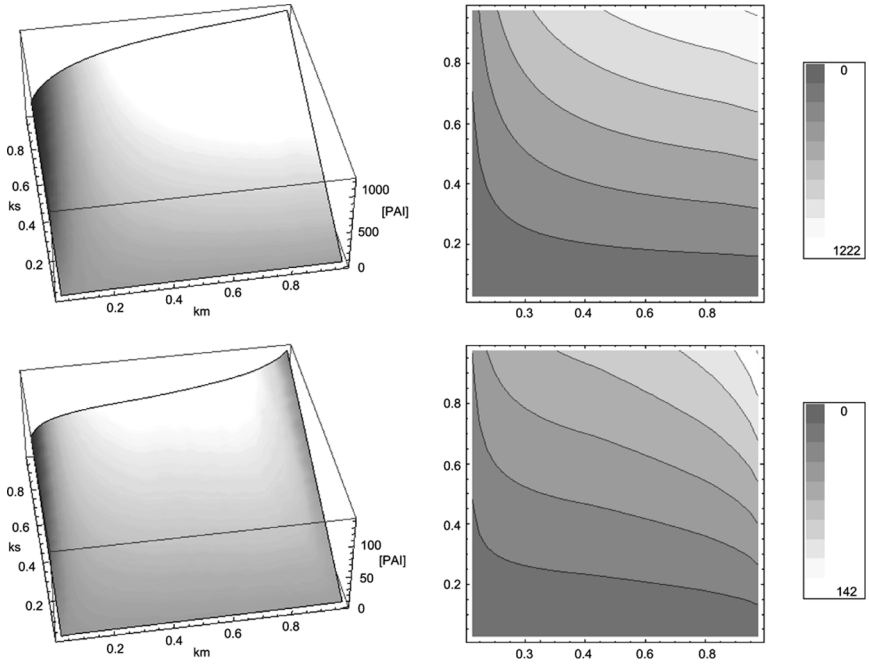

FIGURE 5 Sensitivity analysis of the cellular-automata simulation results: (upper panel) mean and (lower panel) standard deviation of the spatial distribution of matrix-bound PAI-1, with respect to kinetic rates k_m (horizontal axis) and k_s (vertical axis). Increasing k_i would only increase the internalization rate and decrease matrix-bound PAI-1 concentration wherever cells are present; altogether, this would localize peaks of concentration in the outer boundary of the tumor, without changing significantly their average height and standard deviation.

by the set of tumor cells is a collective effect. It allows the internalization flux J_i of a few single cells to reach values which would never be reached if the cells were functioning in isolation. Spontaneously, some cells might benefit from the PAI-1 secretion of the other ones. Locally, J_i might reach values $J_i > J_i^*$ large enough to trigger the mesenchymatous-amoeboid transition of a few single cells and allow their amoeboid move away from the tumor. The stochastic variation of tumor growth and boundary location, self-consistently coupled with PAI-1 reactions, makes this overshoot $J_i > J_i^*$ a random history-dependent event.

This numerical implementation supports the claim that only tumor boundary regions are involved in metastatic escape. It highlights an

emergent situation leading to the spontaneous heterogeneous accumulation of matrix-bound PAI-1 at the tumor boundary, which in turn promotes the amoeboid-mesenchymatous transition and the metastatic escape of a few single cells, selected in a random and history-dependent way. This mechanism accounts for both the possibility and the rarity of mesenchymatous-amoeboid transition events, and it relies on very few ingredients.

3.3.2. *Agent-Based Simulation*

A cellular-automata model, although introducing cell discreteness and stochastic variation in partial differential equations, could lack realism. A structural stability analysis helps delineate the validity of the model. Inferring possible additional contributions quantitatively is difficult experimentally because of the rarity of the phenomenon. We rather relax the hypotheses and simplifications underpinning the cellular-automata simulation.

Three kinds of entities are now considered: tumor cells, PAI-1 molecules in their three different forms, and additional vitronectine molecules bound to the extracellular matrix and promoting soluble PAI-1 matrix binding upon encounter. Moreover, cells are modeled as autonomous entities evolving in a continuous space and endowed with more realistic behaviors: by contrast to the cellular-automata simulation, cell modeling is now dissociated from the topology of underlying space. Cells can be in one of the following states:

- *Active*: an active cell may proliferate, internalize PAI-1, and release soluble PAI-1; cells are created in this active state.
- *Quiescent*: cells become quiescent if they lack basic nutrients and proliferation is paused; however, they continue to release and internalize PAI-1 molecules.
- *Necrotic*: if environmental conditions are even harsher, cells become necrotic and die.

In modeling the behavior of PAI-1 molecules, we consider the discreteness and the stochastic character of molecular events and of diffusion. We no longer need the mean-field description in terms of smooth deterministic concentration fields considered in both partial differential equations and cellular-automata. Molecules of vitronectine are described on average, in terms of a local concentration of molecules in each cell of a regular grid. Molecules of PAI-1 are modeled as autonomous agents produced and released by cells. These molecules can be in one of the aforementioned states: internal, soluble (either

active or inactivated), or matrix-bound (when entering a cell-free region with a sufficient concentration of vitronectine so that it encounters a vitronectine molecule almost surely and binds to it); in the soluble state, they diffuse according to a random walk into the extracellular medium. Molecules of vitronectine have neither active behavior nor diffusive motion (for this reason they are not modeled individually), but their concentration in a given grid cell is updated each time a PAI-1 molecule gets bound to the matrix in this grid cell.

Starting from a single active mesenchymatous cell, from an homogeneous distribution of vitronectine, and in the absence of matrix-bound PAI-1, the agent-based simulation produces a final state in which the initial cell has generated a full-grown tumor, surrounded by an irregular accumulation of molecules of matrix-bound PAI-1. This observation *in-silico* holds true for a wide range of kinetics and parameter settings, a fact which testifies for the robustness of the model. It may also indicate a robustness of the phenomenon itself with respect to change in the surrounding conditions or in any metabolic or signaling factor influencing the parameters (Lesne, 2008). Our numerical results suggest that:

- *The amount of matrix-bound PAI-1 in a given location on the tumor border varies greatly in time*; this comes from an alternation of phases during which PAI-1 accumulates by binding to a cell-free extracellular matrix (through forming a complex with vitronectine) and phases during which, because of tumor growth, one or more cells come in contact and internalize matrix-bound PAI-1; vitronectine molecules do not appear here as a limiting factor. This justifies their omission in the model with partial differential equations or in the cellular automata simulation;
- *The amount of matrix-bound PAI-1 varies greatly from one point to another along the tumor border*; this comes from the fact that the tumor growth is not spatially homogeneous and does not occur simultaneously all around the tumor;
- *The amount of matrix-bound PAI-1 is inversely correlated to the speed of the tumor growth*: the slower the proliferation, the longer the phases during which matrix-bound PAI-1 can accumulate; this suggests that the environment of the tumor, by differentially influencing tumor growth (Hoehme and Drasdo, 2010/this issue), may play a major role in the onset of amoeboid escape.

This agent-based simulation mimics the appearance of a necrotic core while proliferation activity is highest at the tumor boundary; it also shows a spontaneous and heterogeneous accumulation of matrix-bound PAI-1 in the outer shell of the tumor. When the simulation is performed

with simpler rules, in a mean-field approximation in which the growing tumor is assumed to keep a circular shape and the secretion of PAI-1 is homogeneous, no such strong heterogeneities appear in the PAI-1 ring around the tumor (low variance in the ring concentration, data not shown): this confirms the result of the cellular-automata simulation that fluctuations in the shape of the tumor boundary as it grows, originating from the random cell divisions, play en essential role in the distribution of matrix-bound PAI-1 molecules (Figure 6).

4. INSIGHTS FROM BIFURCATION THEORY

4.1. PAI-1-Controlled Bifurcation Diagram

Our numerical simulations favor the explanation that both the metastatic escape and its rarity originate in the control by the internalization flux of matrix-bound PAI-1 of the switch between mesenchymatous and amoeboid states. We suggest a scenario accounting for the molecular, cellular, extracellular, and population features of metastatic escape and secondary tumor growth.

A first option is to implement an extended agent-based simulation of the context-dependent transformations of *all* tumor cells, their migratory motions, their divisions, their interactions with their surroundings and metabolic changes as they move. Such an extensive simulation could include a wealth of ingredients presumably at work in the real system; its quality would be to use raw and elementary ingredients directly. It however does clarify neither the appearance of secondary tumors nor the major mechanisms. The parameters are too many to perform any sensitivity or structural stability analysis.

That is why we focus on the fate of one of the privileged cells having encountered a supra-threshold concentration of matrix-bound PAI-1 and experienced the mesenchymatous-amoeboid transition. The modification of its micro-environment due to neighboring cells (including itself) will be tracked and taken into account *effectively*, through its consequence on the concentration c_m of matrix-bound PAI-1 at the cell location or still more effectively through its consequence on the PAI-1 internalization flux J_i of the selected cell. The experimental investigation of the mesenchymatous-amoeboid transition, Figure 2, led us to formulate our main claim that this cell change is not due to accumulated mutations but to a change in the physiological state of the cell, that is, to a *bifurcation in the intracellular dynamics*. The metabolic network formed with all the species and pathways connected to PAI-1 or PAI-1-regulated reactions experiences a qualitative change of regime, with observable consequences on the cell state in the form of a bi-stable switch.

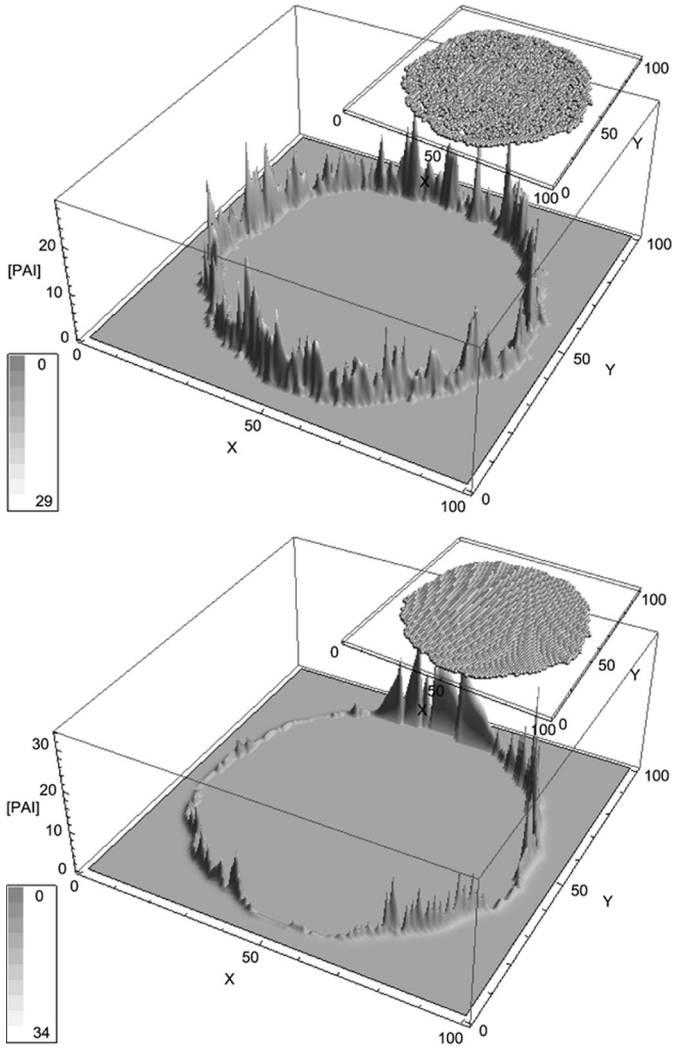

FIGURE 6 Comparison of the (top) agent-based and (bottom) cellular-automata simulation results. Both simulations support the spontaneous heterogeneous accumulation of matrix-bound PAI-1 at the tumor boundary. In the agent-based simulation, the tumor growth results from physiological reactions; it results from a random choice of the dividing cell in the cellular-automata simulation. Here this choice is constrained by enforcing the final shape in order to obtain a tumor geometry comparable to the one obtained in the agent-based simulation. The difference with Figure 4, in which the simulation follows a plain random growth as described in Section 3.3.1, shows that both tumor growth history and geometry matter.

The generic instance of first-order bi-stability (associated with a discontinuous transition between two stable states) is the S-shaped diagram (Ruelle, 1989) sketched on Figure 7. The horizontal axis represents the control parameter, here the concentration c_m of matrix-bound PAI-1 at the cell location or the internalization flux J_i related to c_m through Eq. (5). The vertical axis represents a quantitative feature discriminating the mesenchymatous and amoeboid states and affected in the mesenchymatous-amoeboid transition, notably:

- the cell morphology (observed shape, organization of the cytoskeleton, blebs appearing as J_i increases);
- the nature of the adherence points with or without integrins; the contribution of integrins decreases as J_i increases, replaced by a PAI-dependent mechanism (Czekay and Loskutoff, 2004);
- the force of adherence exerted by the cell, decreasing as J_i increases;
- the cell proteolytic activity (decreasing as J_i increases); and

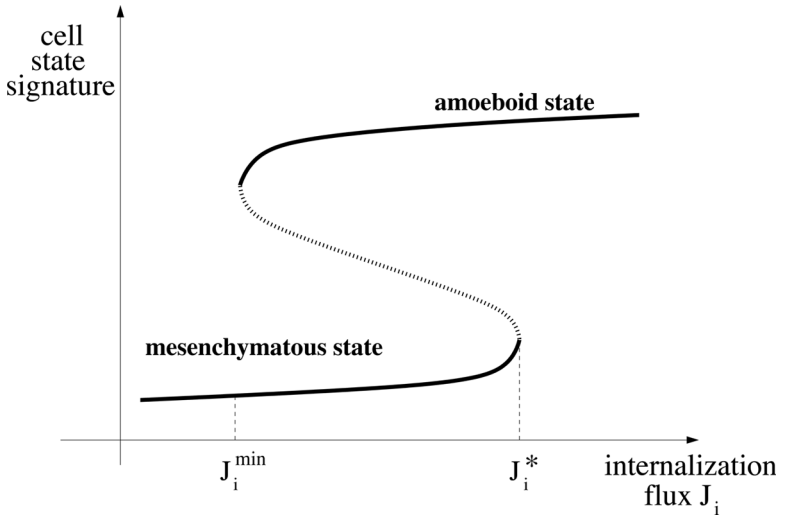

FIGURE 7 Generic bifurcation diagram of a bi-stable switch, here the transition between the mesenchymatous state (lower branch of the S-shaped curve) and the amoeboid state (upper branch) for a given cell as the internalization flux J_i of matrix-bound PAI-1 varies (horizontal axis); this flux is proportional to the concentration of matrix-bound PAI-1 at the cell location and triggers several intracellular pathways responsible for the transition. The vertical axis represents any quantitative feature discriminating the two states.

- the activation or inhibition of internal pathways related to PAI-1, typically the RhoA pathway, involving ROCK activation as J_i increases (Sanz-Moreno et al., 2008; McCarthy, 2009).

The S-shaped curve represents the possible states of a tumor cell in this plane, with bi-stability in a horizontal range $[J_i^{\min},\ J_i^*]$. The lower branch corresponds to the mesenchymatous state and the upper branch to the amoeboid state. We are dealing with dynamic states, which are stable in the sense that they persist and correspond to stationary features. The intermediary dotted branch is unstable. This bifurcation diagram represents the abrupt mesenchymatous-amoeboid transition for $J_i = J_i^*$; the mesenchymatous state no longer exists for $J_i > J_i^*$. It also predicts the occurrence of a reverse transition, the amoeboid-mesenchymatous one, when J_i has decreased back to a value $J_i^{\min}$ smaller than J_i^*. This S-shaped bifurcation is termed *subcritical bifurcation* to indicate that the amoeboid-state domain of existence and stability, in the control parameter space, overlaps the mesenchymatous-state domain of existence and stability, and covers a region $[J_i^{\min},\ J_i^*]$ below the bifurcation threshold J_i^*. Such a bifurcation diagram relies on the property that the threshold for triggering the mesenchymatous-amoeboid transition is higher than the threshold required to simply maintain the amoeboid state once it is established. Reducing to a "plane" diagram (codimension one) is justified by the generic irrelevance of stable components of the dynamics near the bifurcation point: the observed qualitative change is controlled by the parameter which is at the stability threshold, here the concentration of matrix-bound PAI-1, while other parameters and factors are inessential. These arguments do not completely rule out the possibility of a nongeneric, higher-dimensional, and more complex bifurcation diagram but we have no experimental clue on such a situation nor any inconsistency in our scenario requiring to envision a more complex diagram.

This bifurcation viewpoint integrates the exclusive proliferative and migratory capacities of the metastatic cells: the concentration of matrix-bound PAI-1 (which directly controls the internalization flux J_i) is critical in the choice between migration and proliferation, with a higher threshold for the transition from proliferation to migration than for the transition from migration to proliferation. Such a subcritical nature, supported by the first-order character of the transition from mesenchymatous to amoeboid states, suggests a protocol for observing the amoeboid-mesenchymatous transition at a decreasing concentration c_m, which is the quantity monitored in *in vitro* experiments (Malo et al., 2006). The description in terms of a bifurcation

diagram (Figure 7) predicts the reversibility of the transition between the mesenchymatous and amoeboid states. By contrast, mutation-driven transitions are irreversible. We explored this transition and its control (Figure 8) to show the existence of the reverse transition from amoeboid to mesenchymatous state. This allows us to reject scenarios of metastatic escape where a few cells gain migratory ability from accumulated mutations and where most cells of the tumor display no such mutations. We validate the bifurcation diagram, and prove both the reverse transition threshold $c_m^{\min} > 0$ and the fact that it is lower than the threshold for the direct transition $c_m^{\min} < c_m^*$. The cell state is resilient and recovers the mesenchymatous state at low matrix-bound PAI-1 concentration $c < c_m^{\min}$.

4.2. Metastatic Cycle

A cycle is usually associated with the subcritical bifurcation diagram on Figure 7, and we suggest a scenario of the recurrent hiving-fixation-growth cycle generating secondary tumors.

History- and geometry-dependent heterogeneities in the concentration c_m of matrix-bound PAI-1 could build up at the boundary of

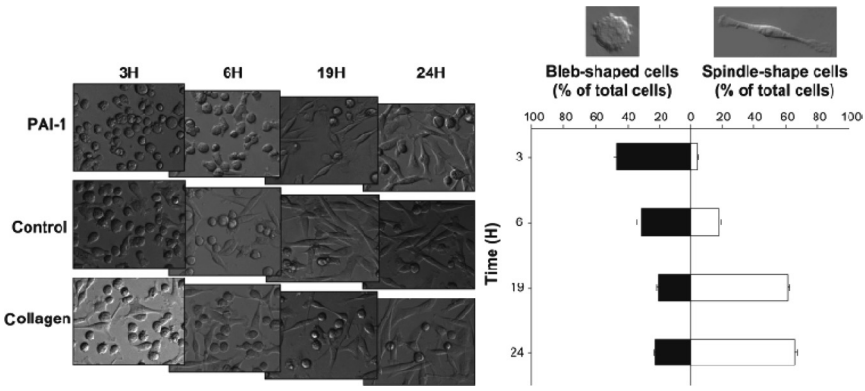

FIGURE 8 (Left) Time-lapse photography of cells seeded on PAI-1 or collagen substrate; bleb-shaped cells becoming elongated show the reversibility of the mesenchymatous-amoeboid transition. (Right) The proportion of bleb- and spindle-shaped MDA-MB-231 breast cancer cells seeded on a weakly PAI-1-enriched micro-environment ($20\,\mu g/cm^2$, below the threshold of the mesenchymatous-amoeboid transition) is shown at successive time points (3, 6, 19, 24 hr). The proportion of bleb-shaped cells (horizontal axis) decreases in favor of spindle-shaped morphology indicating that a reverse amoeboid-mesenchymatous transition takes place.

a proliferating tumor. A mesenchymatous cell reaching one of these privileged locations would follow the lower branch up to the critical value c_m^* at which it switches to the upper branch into the amoeboid state. After switching to the amoeboid state, a cell starts to migrate away from the tumor. Before entering a proliferative state, a migrating cell into the amoeboid state has first to stop and settle, and its metabolic and transcriptional states shift to a regime of growth and division. We saw that such a transition back to the mesenchymatous state could be promoted by the surrounding. The diffusion-limited concentration of soluble PAI-1 decreases as the distance from the tumor cells producing PAI-1 increases, and so does the concentration of its matrix-bound form. The escaping cell soon reaches regions where the concentration of matrix-bound PAI-1 is low. This lowers its internalization flux J_i. Moreover, due to a negative self-regulation of the expression of PAI-1 at the transcription level, the secretion of PAI-1 is reduced in the amoeboid state (while being maximal in the mesenchymatous state). The migrating cell cannot by itself modify its micro-environment into a track covered with a high quantity of matrix-bound PAI-1. Subsequently, the amoeboid state cannot be sustained and the cell switches back to the mesenchymatous state. It could then resume proliferating and generate a metastasis. As the secondary tumor grows, the same metastatic cycle could occur for a small fraction of its cells. Figure 9 represents how the metastatic cycle could originate in an intrinsic hysteretic cycle between two states for a single cell (bold lines). The point is that the control parameter c_m is not tuned from outside but that its variations reflect the modifications of the cell micro-environment during proliferation and migration.

After a few metastatic cycles, the newly born metastasis is far enough from the original tumor and its cells descend from a minute fraction of the cells of the primary tumor, in agreement to *in vivo* observations. The metastatic escape of a single cell is in fact the consequence of a collective effect involving many cells, mainly through their contributions to the release of PAI-1 in the extracellular medium and fixation to the matrix: the consequence is observed at a single cell level but originates at the cell population level. The probability that an escaping metastatic cell reaches blood increases at each cycle, opening the way to other modes of metastatic processes.

4.3. Quasi-Stationary or Transient Cell States

We described the cell trajectory as a succession of well-defined states controlled by the local concentration c_m of matrix-bound PAI-1 or

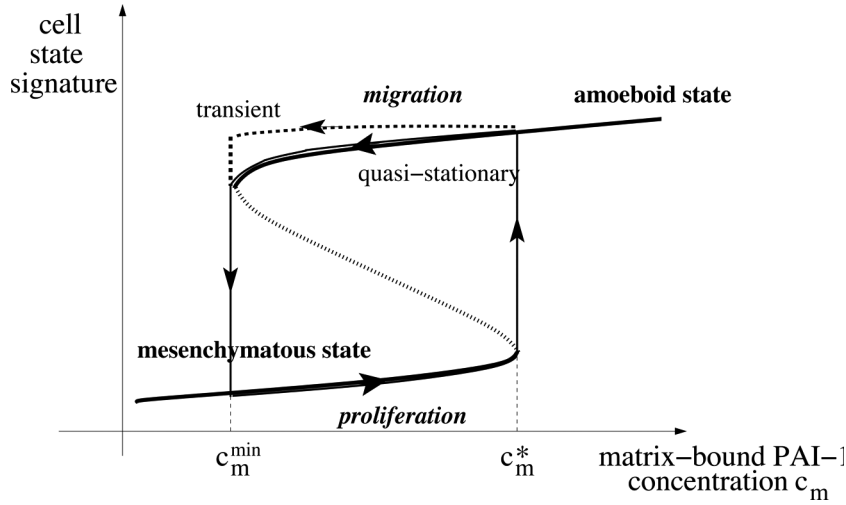

FIGURE 9 Metastatic cycle. The control parameter is the local and instantaneous value c_m of the concentration of matrix-bound PAI-1 at the cell location. The bold lines represent the stable states and the dotted one the unstable branch (bifurcation diagram as in Figure 7); the dashed line represents the typical path of the cell-state trajectory when the quasi-approximation is no longer valid and c_m varies before the cell has relaxed toward the stable branch.

equivalently by the instantaneous value J_i of the cell internalization flux of PAI-1. This paradoxical description (a succession of stationary states), called "quasi-stationary approximation" (also "adiabatic approximation" in physics), is justified by the difference between the time scale of the modification of the micro-environment (and the ensuing modification of c_m and J_i) and the faster time scale of the cell response: the cell is almost always observed in a stationary state, following the stable branches of the bifurcation diagram as c_m or J_i vary slowly.

When this quasi-stationary approximation is no longer true, for instance in the presence of memory or slow relaxation, the bifurcation diagram still provides bounds and qualitative guidelines on the trajectory of the cell state. Consider for instance an amoeboid cell reaching a region poor in PAI-1, with $c_m < c_m^*$. If a non negligible duration (compared to other relevant characteristic times) is required before the PAI-1 signal comes down, the cell relaxes to the mesenchymatous state with a delay: it first remains in a transient regime and its trajectory, represented by the dashed line on Figure 9, then deviates

from the branches of stationary states forming the S-shaped curve. This trajectory depends on the cell history, but lies above the upper branch. Whether the cell behavior is an adiabatic response following a stable branch of the bifurcation diagram or an out-of-equilibrium response depends on the relative values of the characteristic time of variation of the value c_m at the cell location (which corresponds to the characteristic time of migration toward the region poor in matrix-bound PAI-1 and depends on both the gradient of matrix-bound PAI-1 and the migration velocity) and the characteristic time of relaxation of the PAI-1-signaling activity triggered by the passage of the cell into a region rich in matrix-bound PAI-1.

No specific genetic mutation is necessary to explain the metastatic cycle, where the passage from the mesenchymatous to the amoeboid state is a bifurcation rather than an event triggered by a mutation. The reverse transition for the *same* cell when external conditions have changed enough would be hard to observe if the transition were determined genetically. Our scenario does not conflict with the accumulation of mutations associated with the metastatic process. We suggest that mutations observed in metastatic cells are neither specific to these cells nor sufficient to explain the move away from the tumor. In our scenario, tumor cells are genetically identical but made functionally different by their different micro-environments. The mutations arising as cancer develops and tumor ages are shared by a large fraction of tumor boundary cells. They are likely to change the bifurcation diagram. Only a few candidates selected among the population of mutant cells by a dynamic and multilevel process move away. We predict that cells in a nascent secondary tumor and cells at the outer boundary of the primary tumor have the same genome and mutation load.

4.4. Oncogenesis and Metastatic Catastrophe

Describing changes of metastatic features during the progression of cancer requires to situate normal or early cancer cells (having just experienced the epithelial-mesenchymatous transition). The bifurcation diagram of Figure 7 is completed in a 3-dimensional space by a third axis Z representing the cell type. It represents the topological changes altering the S-shaped bifurcation diagram as the cell type is modified during oncogenesis, mainly by accumulating mutations: a relevant choice for Z is the total number of mutations. Thom (1975) established the possible generic changes in a bifurcation diagram seen as various singularities of the corresponding hypersurface

(here a two-dimensional surface, with S-shaped section, in a three-dimensional space {(*X, Y, Z*)}). He termed "catastrophes" these generic singularities. In the present case, either:

1. The bifurcation diagram on Figure 7 is qualitatively the same for normal cells, early cancer cells, and advanced tumor cells. This means that both thresholds J_i^* and $J_i^{\min}$ exist, keeping finite and distinct values when the cancerous stage of the cell changes.
2. No such bi-stability exists for normal cells, where a single stable state would change continuously as J_i increases. Genericity ensures that the bi-stability observed for cancer cells arises through a *fold catastrophe* (Thom, 1975), as represented on Figure 10.

The failure to observe the mesenchymatous-amoeboid transition for normal cells prevents one from discriminating the two cases.

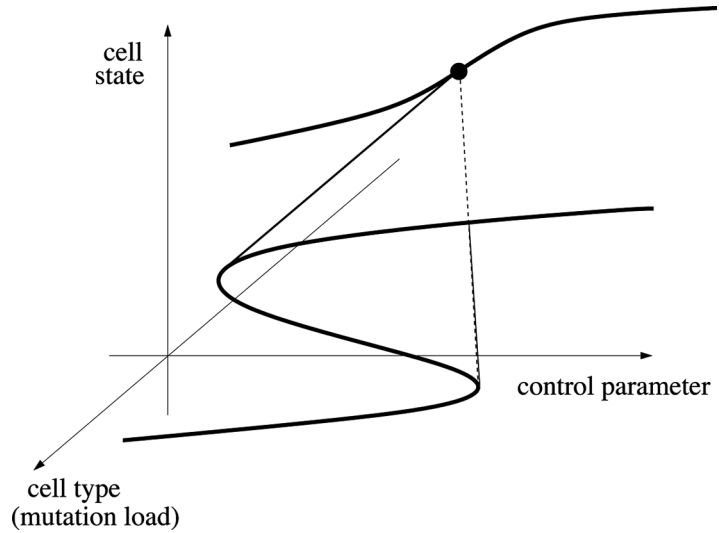

FIGURE 10 Bifurcation diagram of Figure 7 in a 3-dimensional space. The *X*-axis is the control parameter, namely the internalization flux J_i of matrix-bound PAI-1, controlled itself by the concentration c_m of matrix-bound PAI-1 at the cell location. The *Y*-axis represents any measurable feature of the cell state discriminating mesenchymatous from amoeboid state. The *Z*-axis represents the cell cancerous stage, directly related to its mutation load. Bi-stability arising as the surface folds onto itself (fold catastrophe) occurs—in the scenario—only for the cells having the sufficient total number of cancerous features.

Perhaps the first case holds true and the threshold for the mesenchymatous-amoeboid transition cannot be reached in normal and in early cancer cells, either because the value J_i^* is greater than in cancer cells, or because the concentration c_m of matrix-bound PAI-1 cannot reach high enough values around normal cells, or because their rate of internalization k_i (such that $J_i = k_i c_m$) is too low. The rate k_i depends on the total number and the activity of uPA receptors, which are known to be far higher in cancer cells, all the more so that cancer is advanced. During oncogenesis, k_i increases and PAI-1 is released by the cells, expectedly surrounded with higher c_m values. This is enough to explain how cancer cells can have higher internalization flux. The second case is described by a three-dimensional extension of the bifurcation diagram into a fold catastrophe. The third dimension is associated with long-term biological evolution and accumulation of mutations, leading to metastatic potentialities in agreement with the cancer multistage theory (Gerstung and Beerenwinkel, 2010/this issue). A main result of catastrophe theory is the existence of only a few archetypal ways of fixed-point destabilization as the dynamics varies, here the "fold" type represented on Figure 10. Right after the catastrophe, J_i^* and $J_i^{\min}$ are close to each other; they coincide at the catastrophe point. The difference between the two stable states in the bi-stable region is weak: if a mesenchymatous-amoeboid transition occurs, the cell shows only a transient bleb-shaped morphology, with no consequence. In particular, the cell remains in the amoeboid state too briefly to have a metastatic escape. Preliminary qualitative experiments (Cartier-Michaud et al., unpublished results) bring some evidence to such behavior. Further experiments are necessary to discriminate the two cases for the bifurcation landscape.

Another matter is to describe the joint dynamics of the cell physiological state (Y), control parameter (X), and cell genetic state (Z), in order to obtain a scenario at the cell population level with possible collectively-driven and out-of-equilibrium behavior at the cell level. For instance, in any bi-stable situation, the time variation of J_i determines the observed behavior entirely, depending on whether J_i reaches J_i^* or not. If it reaches J_i^*, does it reach $J_i^{\min}$ back or not, leading either to a restricted back-and-forth motion on a single stable branch or to a full cycle? Time scale and the range of variation of J_i determine whether the motion follows the stable branches adiabatically or behaves out of equilibrium. In any case, a therapeutic target consists of modifying the bifurcation diagram so as to weaken its metastatic possibilities and the efficiency of the metastatic cycle.

5. CONCLUSION

Our scenario of metastatic process builds on a novel idea: although the accumulation of mutations plays an essential role in the metastatic process, the actual determination of the cell experiencing a metastatic escape is the consequence of a complex sequence of stochastic and multi-scale events involving a whole population of "potentially metastatic" cells all displaying the same mutation load. Agent-based simulation, cellular automata, bifurcation theory, and catastrophe theory jointly capture the interplay between different levels and the role of stochastic variation and history.

We first showed numerically that collectively induced heterogeneities in the concentration of matrix-bound PAI-1 can develop and induce the transition of a few cells to the migratory-prone amoeboid state. Our scenario is based on an experimentally supported alternation of mesenchymatous and amoeboid states, corresponding respectively to the proliferation and migration of a few cells. They are selected among other cells of the population by a rare, stochastic, and history-dependent conjunction of molecular events. This scenario is a cellular version of hiving: amoeboid migration involves a small number of cells and is a transient stage during which cells exchange their proliferative capacities against migratory abilities. We suggest that all cells of the outer shell of the tumor contribute to this process because their mutualized production of PAI-1 is necessary to trigger the transition to the amoeboid state of a few cells. All cells of the outer shell of the tumor have the same metastatic potentiality on genetic grounds, but only those encountering a localized accumulation of matrix-bound PAI-1 will be able to express this potentiality. A single species, PAI-1, would coordinate events at different scales, from molecular determinants up to the consequences for the tissue. The metastatic cycle would involve both intra-cellular and extracellular processes, as well as a collective modification of the micro-environment, in agreement with recent observations (Albini et al., 2008; Bidard et al., 2008). Amoeboid migration is too rare and transient to be easily observed *in vivo* or *in vitro* but it is likely to have dramatic consequences on metastatic spreading.

In our scenario, cells modify their micro-environment, which in turn influences the state of some cells through the activation of specific signaling pathways. Because the metastatic process originates from a coordinated alternation of proliferation and migration, it articulates single cells and the cell population. It is difficult to observe this process not only *in vivo* but also *in vitro*. Our scenario articulates available biological facts into a protocol for investigating the mesenchymatous-amoeboid and amoeboid-mesenchymatous transitions with normal

cells and cancer cells taken at different stages after the epithelial-mesenchymatous transition. The purpose is to reconstruct the multivariate bifurcation diagram and discriminate the two possible transformations of the bifurcation diagram along the progression of the cancer. Reducing matrix binding of PAI-1 or modifying another factor so as to decrease k_i or increase the threshold J_i^* of the mesenchymatous-amoeboid transition would reduce the metastatic escape; reducing the synthesis of PAI-1 is not an option because of side effects. Our scenario also suggests to reduce the matrix binding ability of PAI-1, targeting the micro-environment rather than the tumor cells themselves (Whiteside, 2008).

REFERENCES

Albini, A. (2008). Tumor microenvironment, a dangerous society leading to cancer metastasis. From mechanisms to therapy and prevention. *Cancer and Metastasis Reviews*, *27*: 3–4.

Albini, A., Mirisola, V., and Pfeffer, U. (2008). Metastasis signatures: Gene regulating tumor-microenvironment interactions predict metastatic behavior. *Cancer and Metastasis Reviews*, *27*: 75–83.

Berx, G., Raspé, E., Christofori, G., et al. (2007). Pre-EMTing metastasis? Recapitulation of morphogenetic processes in cancer. *Clinical and Experimental Metastasis*, *24*: 587–597.

Bidard, F.C., Pierga, J.Y., Vincent-Salomon, A., and Poupon, M.F. (2008). A class action against the microenvironment: Do cancer cells cooperate in metastasis? *Cancer and Metastasis Reviews*, *27*: 5–10.

Biermann, J.C., Holzscheiter, L., Kotzsch, M., et al. (2008). Quantitative RT-PCR assays for the determination of urokinase-type plasminogen activator and plasminogen activator inhibitor type 1 mRNA in primary tumor tissue of breast cancer patients: Comparison to antigen quantification by ELISA. *International Journal of Molecular Medicine*, *21*: 251–259.

Castelló, R., Landete, J.M., España, F., et al. (2007). Expression of plasminogen activator inhibitors type 1 and type 3 and urokinase plasminogen activator protein and mRNA in breast cancer. *Thrombosis Research*, *120*: 753–762.

Chazaud, B., Bonavaud, S., Plonquet, A., et al. (2000). Involvement of the [uPAR:uPA:PAI-1:LRP] complex in human myogenic cell motility. *Experimental Cell Research*, *258*: 237–244.

Chazaud, B., Ricoux, R., Christov, C., et al. (2002). Promigratory effect of plasminogen activator inhibitor-1 on invasive breast cancer cell populations. *American Journal of Pathology*, *160*: 237–246.

Czekay, R.P. and Loskutoff, D.J. (2004). Unexpected role of plasminogen activator inhibitor 1 in cell adhesion and detachment. *Experimental Biology and Medecine, (Maywood)*, *229*: 1090–1096.

Friedl, P. (2004). Pre-specification and plasticity: Shifting mechanisms of cell migration. *Current Opinions in Cell Biology*, *16*: 14–23.

Friedl, P. and Wolf, K. (2003). Tumour-cell invasion and migration: Diversity and escape mechanisms. *Nature Reviews Cancer*, *3*: 362–374.

Gavert, N. and Ben-Ze'ev, A. (2008). Epithelial-mesenchymal transition and the invasive potential of tumors. *Trends in Molecular Medecine*, *14*: 199–209.

Gerstung, M. and Beerenwinkel, N. (2010/this issue). Waiting time models of cancer progression. *Mathematical Population Studies*, *17*: 115–135.

Hoehme, S. and Drasdo, D. (2010/this issue). Biomechanical and nutrient controls in the growth of mammalian cell populations. *Mathematical Population Studies*, *17*: 166–187.

Jänicke, F., Prechtl, A., Thomssen, C., et al. (2001). Randomized adjuvant chemotherapy trial in high-risk, lymph node-negative breast cancer patients identified by urokinase-type plasminogen activator and plasminogen activator inhibitor type 1. *Journal of the National Cancer Institute*, *93*: 913–920.

Landau, L.D. and Lifshitz, E.M. (1959). *Fluid Mechanics*. London: Pergamon Press.

Lesne, A. (2007). Discrete vs continuous controversy in physics. *Mathematical Structure in Computer Science*, *17*: 185–223.

Lesne, A. (2008). Robustness: Confronting lessons from physics and biology. *Biological Reviews*, *83*: 509–532.

Look, M.P., van Putten, W.L.J., Duffy, M.J., et al. (2002). Pooled analysis of prognostic impact of urokinase-type plasminogen activator and its inhibitor PAI-1 in 8377 breast cancer patients. *Journal of the National Cancer Institute*, *94*: 116–128.

Malo, M., Charrière-Bertrand, C., Chettaoui, C., et al. (2006). The PAI-1 swing: Microenvironment and cancer cell migration. *Comptes Rendus Biologie*, *329*: 919–927.

McCarthy, N. (2009). Metastasis: Moved to act. *Nature Reviews Cancer*, *9*: 3.

Pedersen, T.X., Pennington, C.J., Almholt, K., et al. (2005). Extracellular protease mRNAs are predominantly expressed in the stromal areas of microdissected mouse breast carcinomas. *Carcinogenesis*, *26*: 1233–1240.

Ruelle, D. (1989). *Elements of Differentiable Dynamics and Bifurcation Theory*. New York: Academic Press.

Sanz-Moreno, V., Gadea, G., Ahn, J., et al. (2008). Rac activation and inactivation control plasticity of tumor cell movement. *Cell*, *135*: 510–523.

Taylor, J., Hickson, J., and Lotan, T. (2008). Using metastasis suppressor proteins to dissect interactions among cancer cells and their microenvironment. *Cancer and Metastasis Reviews*, *27*: 67–73.

Thiery, J.P. (2002). Epithelial-mesenchymal transitions in tumor progression. *Nature Reviews Cancer*, *2*: 442–454.

Thom, R. (1975). *Structural Stability and Morphogenesis*. Reading, MA: Benjamin Addison Wesley.

Vincan, E., Brabletz, T., Faux, M.C., and Ramsay, R.G. (2007). A human three-dimensional cell line model allows the study of dynamic and reversible epithelial-mesenchymal and mesenchymal-epithelial transition that underpins colorectal carcinogenesis. *Cells Tissues Organs*, *185*: 20–28.

Whiteside, T.L. (2008). The tumor microenvironment and its role in promoting tumor growth. *Oncogene*, *27*: 5904–5912.

Wilkins-Port, C.E. and Higgins, P.J. (2007). Regulation of extracellular matrix remodelling following transforming growth factor-beta1/epidermal growth factor-stimulated epithelial-mesenchymal transition in human premalignant keratinocytes. *Cells Tissues Organs*, *185*: 116–122.

Wilkins-Port, C.E., Higgins, C.E., Freytag, J., et al. (2007). PAI-1 is a critical upstream regulator of the TGF-β1/EGF-induced invasive phenotype in mutant p53 human cutaneous squamous cell carcinoma. *Journal of Biomedicine and Biotechnology*, *85208*. doi: 10.1155/2007/85208

Witz, I.P. (2008). Tumor-microenvironment interactions: Dangerous liaisons. *Advances in Cancer Research*, *100*: 203–229.